



Lab Resource: Genetically-Modified Multiple Cell Lines



Generation of two induced pluripotent stem cell lines and the corresponding isogenic controls from Parkinson's disease patients carrying the heterozygous mutations c.815G > A (p.R272Q) or c.1348C > T (p.R450C) in the RHOT1 gene encoding Miro1

Axel Chemla^a, Giuseppe Arena^{a,*}, Gizem Onal^{b,c,d}, Jonas Walter^{e,1}, Clara Berenguer-Escuder^a, Dajana Grossmann^{a,f}, Anne Grünwald^{g,h}, Jens C. Schwamborn^e, Rejko Krüger^{a,i,j,*}

^a Translational Neuroscience, Luxembourg Centre for Systems Biomedicine (LCSB), University of Luxembourg, Luxembourg

^b Department of Physiology, Anatomy and Genetics, University of Oxford, UK

^c Kavli Institute for Nanoscience Discovery, University of Oxford, UK

^d Department of Medical Biology, Faculty of Medicine, Balikesir University, Turkey

^e Developmental and Cellular Biology, Luxembourg Centre for Systems Biomedicine (LCSB), University of Luxembourg, Luxembourg

^f Translational Neurodegeneration Section "Albrecht-Kossel", Department of Neurology, University Medical Center Rostock, University of Rostock, Rostock, Germany

^g Molecular and Functional Neurobiology, Luxembourg Centre for Systems Biomedicine (LCSB), University of Luxembourg, Luxembourg

^h Institute of Neurogenetics, University of Lübeck, Lübeck, Germany

ⁱ Centre Hospitalier de Luxembourg, Luxembourg

^j Transversal Translational Medicine, Luxembourg Institute of Health (LIH), Luxembourg

ABSTRACT

Fibroblasts from two Parkinson's disease (PD) patients carrying either the heterozygous mutation c.815G > A (Miro1 p.R272Q) or c.1348C > T (Miro1 p.R450C) in the RHOT1 gene, were converted into induced pluripotent stem cells (iPSCs) using RNA-based and episomal reprogramming, respectively. The corresponding isogenic gene-corrected lines have been generated using CRISPR/Cas9 technology. These two isogenic pairs will be used to study Miro1-related molecular mechanisms underlying neurodegeneration in relevant iPSC-derived neuronal models (e.g., midbrain dopaminergic neurons and astrocytes).

1. Resource table

(continued)

Unique stem cell line identifier	1. LCSBi009-A 2. LCSBi009-A-1 3. LCSBi010-A 4. LCSBi010-A-1 5. LCSBi010-A-2
Alternative name(s) of stem cell line	1. RHOT1_R272Q_clone1_PD 2. RHOT1_R272Q_clone18_IsogenicControl 3. RHOT1_R450C_clone5_PD 4. RHOT1_R450C_clone6_IsogenicControl 5. RHOT1_R450C_clone10_IsogenicControl
Institution	Luxembourg Centre for Systems Biomedicine (LCSB), University of Luxembourg, Luxembourg

(continued on next column)

Contact information of the reported cell line distributor	Prof. Rejko Krüger; rejko.krueger@uni.lu
Type of cell line	iPSCs
Origin	Human
Additional origin info (applicable for human ESC or iPSC)	1. Age at biopsy: 78 years Sex: female Ethnicity: European White 2. As in 1. 3. Age at biopsy: 54 years Sex: female Ethnicity: European White 4. As in 3. 5. As in 3
Cell Source	Dermal fibroblasts

(continued on next page)

* Corresponding authors at: Translational Neuroscience team, Luxembourg Centre for Systems Biomedicine (LCSB), University of Luxembourg, Campus Belval, 6 Avenue du Swing, L-4367 Esch-sur-Alzette, Luxembourg.

E-mail addresses: Giuseppe.Arena@uni.lu (G. Arena), Rejko.Krueger@lih.lu (R. Krüger).

¹ Current address: Department of Proteomics, The Novo Nordisk Foundation Center for Protein Research, Faculty of Health and Medical Sciences, University of Copenhagen, Blegdamsvej 3B, Copenhagen 2200, Denmark.

<https://doi.org/10.1016/j.scr.2023.103145>

Received 3 April 2023; Received in revised form 9 June 2023; Accepted 12 June 2023

Available online 14 June 2023

1873-5061/© 2023 The Author(s). Published by Elsevier B.V. This is an open access article under the CC BY license (<http://creativecommons.org/licenses/by/4.0/>).

(continued)

Method of reprogramming	<i>RHOT1_R272Q</i> : RNA transfection <i>RHOT1_R450C</i> : nucleofection of episomal reprogramming vectors
Clonality	Clonal
Evidence of the reprogramming transgene loss (including genomic copy if applicable)	Loss of episomal reprogramming vectors (<i>RHOT1_R450C</i> only)
The cell culture system used	iPSCs were maintained under feeder-free conditions, on Matrigel-coated wells, in presence of Essential 8™ (E8) medium
Type of the Genetic Modification	Spontaneous point mutation (LCSBi009-A and LCSBi010-A) Gene correction (LCSBi009-A-1, LCSBi010-A-1 and LCSBi010-A-2)
Associated disease	Parkinson disease (OMIM #168600)
Gene/locus	<i>RHOT1</i> (17q11.2), Gene ID: 55,288
Method of modification / user-customisable nuclease (UCN) used, the resource used for design optimisation	CRISPR/Cas9
User-customisable nuclease (UCN) delivery method	Nucleofection
All double-stranded DNA genetic material molecules introduced into the cells	Yamanaka reprogramming vectors, SpCas9 plasmid
Analysis of the nuclease-targeted allele status	Sanger Sequencing of the targeted alleles
Method of the off-target nuclease activity prediction and surveillance	The Benchling CRISPR design tool was used to assess on- and off-target potential of selected guide RNA sequences
Descriptive name of the transgene	N/A
Eukaryotic selective agent resistance cassettes	N/A

(continued on next column)

(continued)

(including inducible, gene/cell type-specific)	
Inducible/constitutive expression system details	N/A
Date archived/stock creation date	01.12.2022
Cell line repository/bank	https://hpscereg.eu/cell-line/LCSBi009-A https://hpscereg.eu/cell-line/LCSBi010-A-1 https://hpscereg.eu/cell-line/LCSBi010-A-1 https://hpscereg.eu/cell-line/LCSBi010-A-2
Ethical/GMO work approvals	The Luxembourgish National Research Ethics Committee (CNER) provided ethical approval for the following project: "Disease modelling of Parkinson's disease using patient-derived fibroblasts and induced pluripotent stem cells" (DiMo-PD, CNER #201411/05).
Addgene/public access repository recombinant DNA sources' disclaimers (if applicable)	pCXLE-hUL (Addgene #27080), pCXLE-hSK (Addgene #27078), and pCXLE-hOct3/4 (Addgene #27076)

2. Resource utility

We recently identified distinct PD patients carrying different heterozygous mutations in the *RHOT1* gene encoding Miro1 (Berenguer-Escuder et al., 2019, 2020; Grossmann et al., 2019; Grossmann et al., 2020). Here we report the generation of iPSCs – and the corresponding gene-corrected lines – from two carriers of different PD-associated Miro1 mutations, which can be used to investigate the impact of Miro1 deficiency on PD pathogenesis Table 1.

Table 1
Characterization and validation.

Classification (optional italicized)	Test	Result	Data
Morphology	Photography	Typical iPSC morphology	Fig. 1 panel A
Pluripotency status evidence for the described cell line	Immunocytochemistry	All iPSC clones display a nuclear localization of the pluripotency markers Nanog and Oct3/4	Fig. 1 panel C
	RT-qPCR	All iPSC clones express the pluripotency markers Nanog and Oct3/4	Fig. 1 panel D
Karyotype	-Illumina iScan S/N: N234 -Karyostat+	No aneuploidies detected	Supplementary Fig. 5
Genotyping for the desired genomic alteration/allelic status of the gene of interest	PCR across the edited site or targeted allele-specific PCR [mandatory]	Successful correction of the intended mutations Absence of large deletions in the region targeted by the gRNAs	Fig. 1 panel B Supplementary Fig. 4
	Evaluation of the - (homo-/hetero-/hemi-) zygous status of introduced genomic alteration(s)	N/A	N/A
	Transgene-specific PCR (when applicable)	N/A	N/A
Verification of the absence of random plasmid integration events	PCR/Southern [mandatory]	Loss of reprogramming vectors confirmed	Supplementary Fig. 1
Parental and modified cell line genetic identity evidence	STR analysis	Identical genotypes between parental and gene-edited lines	Supplementary Fig. 6
Mutagenesis / genetic modification outcome analysis	Sanger Sequencing	Confirmation of the homozygous corrections of the mutated alleles and absence of indel mutations	Fig. 1 panel B
	PCR-based analyses	N/A	N/A
	Southern Blot or WGS; western blotting (for knock-outs, KOs)	N/A	N/A
Off-target nuclease activity analysis	Targeted PCR and sequencing for the top 5 predicted off-targets located in genes [Optional but highly-recommended if Cas editing is used]	N/A	N/A
Specific pathogen-free status	Mycoplasma [mandatory]	Negative	Supplementary Fig. 7
Multilineage differentiation potential	Directed differentiation [mandatory]	Ability of all clones to differentiate into the three germ layers	Fig. 1 panel E
Donor screening (OPTIONAL)	HIV 1 + 2 Hepatitis B, Hepatitis C, HTLV 1 + 2	Negative	Supplementary Fig. 7
Genotype - additional histocompatibility info (OPTIONAL)	Blood group genotyping	N/A	N/A
	HLA tissue typing	N/A	N/A

3. Resource details

For the generation of parental iPSC lines (i.e., *LCSBi009-A* and *LCSBi010-A*), we reprogrammed fibroblasts of two PD patients carrying different *RHOT1* heterozygous mutations – the c.815G > A (p.R272Q) and the c.1348C > T (p.R450C) mutation – which are located in the first

EF-hand (EF1) and in the C-terminal GTPase (cGTPase) domain of Miro1, respectively (Grossmann et al., 2019). Miro1 p.R272Q fibroblasts were reprogrammed into iPSCs using a virus-free and integration-free RNA-based approach, consisting in the transfection of a synthetic *in vitro* transcribed RNA replicon expressing the reprogramming factors in a single self-replicating polycistronic transcript. Miro1 p.R450C iPSCs

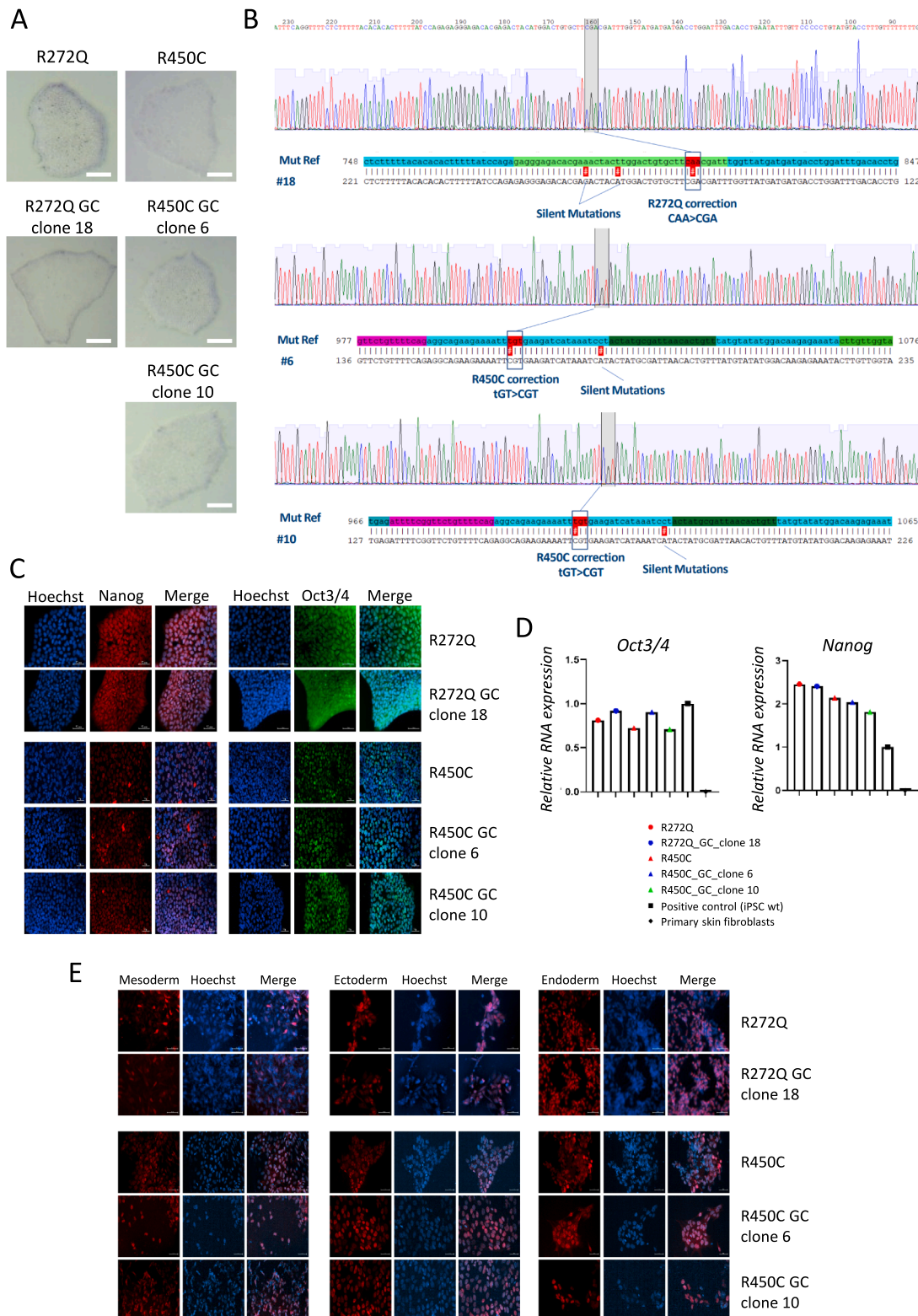


Fig. 1.

were established following electroporation of patient fibroblasts with episomal vectors expressing the four Yamanaka reprogramming factors. Clonal iPSC populations were identified by morphology, isolated and expanded (Fig. 1A, upper panels). The absence of plasmid integration in their genome was confirmed by PCR analysis (Supplementary Fig. 1). Isogenic, gene-corrected lines (i.e., *LCSBi009-A-1*, *LCSBi010-A-1* and *LCSBi010-A-2*) were generated by Axol Bioscience using a CRISPR/Cas9-mediated gene editing approach (Supplementary Figs. 2 and 3). For both Miro1 R272Q and Miro1 R450C gene correction, two distinct gRNAs targeting the intended mutation site were selected based on prior *in silico* analysis considering their distance from the target, predicted activity and off-target profile (Table 2). After testing their cutting efficiency in the corresponding parental iPSC lines, gRNAs of higher activity were chosen (C1917A-R272Q-g2 and C1917B-R450C-g1, respectively). Cas9-

mediated re-cutting was prevented by introducing silent mutations in the gRNA binding sites present on the editing donor, consisting of a single-stranded oligodeoxynucleotide (ssODN) with homology arms flanking the target site (Table 2). Gene editing factors were introduced in the parental iPSC lines by nucleofection. Several iPSC colonies were screened by PCR and Sanger sequencing, confirming the successful corrections and the absence of indel mutations in one Miro1 p.R272Q (clone 18) and in two Miro1 p.R450C (clone 6 and 10) gene-edited clones (Table 2, Fig. 1B). qPCR analysis excluded the presence of large deletions in the region targeted by the respective gRNAs (Supplementary Fig. 4). The three gene-corrected lines, all displaying a typical iPSC morphology (Fig. 1A, lower panels), were then expanded and subjected to further characterization. Immunocytochemistry and RT-qPCR analyses confirmed that both patient-derived and gene-edited clones

Table 2
Reagent details.

Antibodies and stains used for immunocytochemistry/flow-cytometry			
	Antibody	Dilution	Company Cat # and RRID
Pluripotency Markers	Rabbit anti Nanog	1:500	Abcam, Cat #: ab21624; RRID: AB_446437
Pluripotency Markers	Mouse anti Oct3/4	1:1000	Santa Cruz, Cat #: sc-5279; RRID: AB_628051
Secondary antibody	Alexa Fluor 488 Goat anti-Mouse IgG (H + L)	1:1000	Invitrogen, Cat #: A11029; RRID: AB_138404
Secondary antibody	Alexa Fluor 568 Goat anti-Rabbit IgG (H + L)	1:1000	Invitrogen, Cat #: A11036; RRID: AB_143011
Mesoderm Marker	Goat anti Brachyury	1:500	Human Pluripotent Stem Cell Functional Identification Kit (R&D Systems, Cat No. SC027B)
Endoderm Marker	Goat anti SOX-17	1:500	
Ectoderm Marker	Goat anti OTX2	1:500	
Secondary antibody	Alexa Fluor 647 Donkey anti Goat IgG (H + L)	1:1000	Invitrogen, Cat No. A21447; RRID: AB_141844
Site-specific nuclease			
Nuclease information	Nuclease type/version		SpCas9
Delivery method	Nucleofection		Amaxa 4D
Selection/enrichment strategy	Selection cassette(s), FACS		N/A
Primers and Oligonucleotides used in this study			
	Target	Forward/Reverse primer (5'-3')	
Pluripotency Marker (RT-qPCR)	OCT4-FAM	Hs00999632_g1 (Thermo Fisher Scientific)	
Pluripotency Marker (RT-qPCR)	NANOG-FAM	Hs02387400_g1 (Thermo Fisher Scientific)	
Housekeeping gene (RT-qPCR)	ACTB-VIC	Hs03023880_g1 (Thermo Fisher Scientific)	
Potential random integration-detecting PCRs	OriP fw	TTCCACGAGGGTAGTGAACC	
Potential random integration-detecting PCRs	OriP rv	TCGGGGGTGTTAGAGACAAC	
gRNA Miro1 c.815G > A mutation	RHOT1 exon 11	GAGGGAGACACGAACTACT	
gRNA Miro1 c.1348C > T mutation	RHOT1 exon 16	ATTTTCGGTTCTGTTTTTCAG	
Miro1 c.815G > A ssODN repair template	RHOT1 exon 11	GGAACAAATATTCCAGGTGTCAAATCCAGGTCATCATATAACC AAATCGTTCGAAGCACAGTCCATGTAGTCTCTGTCCTCCCTCTCT GGATAAAAAGTGTGTGTA AAAAGAGAAAACTGA	
Miro1 c.1348C > T ssODN repair template	RHOT1 exon 16	TCCATATACATAAACAGTGTAAATCGCATAGTAGGATTTATGA TCTTCACGAAATTTCTCTGTCCTGAAACAGAACCGAAAAAT CTCAATATCTGCAGTAACTAGTTTTCAA	
Screening PCR Miro1 c.815G > A gene-corrected clones	RHOT1 exon 11	GAGGCACAGTGAAGTTAATGAGATTG / CTTTAATCACAGCAATTTGGGAGGC	
Screening PCR Miro1 c.1348C > T gene-corrected clones	RHOT1 exon 16	ATGGTATAATGAAGATTGCCAGCAG / ACCACGCCTAGCCAAAAGAC	
qPCR allelic status Miro1 c.815G > A gene-corrected clones	RHOT1 intron 10	GGCCATTTCTCTAGTGCTC / ATACGGATGCTAGCTTTGCATTG	
qPCR allelic status Miro1 c.1348C > T gene-corrected clones	RHOT1 intron 17	ACTTGTGGTAAGAAATCTGTGGC / CAGAAGTTCTACAGAGAGTCATTCA	
Housekeeping gene (qPCR)	GAPDH	TCTCCTGGAAGGGCTTCGTA / TAAGGCATGGCTGCAACTGA GAGGCACAGTGAAGTTAATGAGATTG	
Sanger sequencing Miro1 c.815G > A gene-corrected clones	RHOT1 exon 11	GAGGCACAGTGAAGTTAATGAGATTG	
Sanger sequencing Miro1 c.1348C > T gene-corrected clones	RHOT1 exon 16	GAACAAATACATCTTTTATTTTAG	

expressed the pluripotency markers OCT3/4 and Nanog (Fig. 1C and D). Moreover, they were all able to differentiate into the three germ layers (Fig. 1E). Finally, all iPSC lines displayed a normal karyotype (Supplementary Fig. 5), were genetically identical to the corresponding fibroblasts (Supplementary Fig. 6) and free of contamination by human pathogens (Supplementary Fig. 7).

4. Materials and methods

4.1. Cell culture and reprogramming

PD patient-derived fibroblasts were grown in DMEM medium containing 4.5 g/L D-glucose, 10% FBS and 1% Pen/Strep (Thermo Fisher Scientific). For the generation of Miro1 p.R272Q iPSCs, fibroblasts were reprogrammed using the Simplicon™ RNA Reprogramming Kit (Merck/EMD Millipore, Cat No. SCR550), according to the manufacturer's instructions. Briefly, cells were pre-treated with the B18R Protein (Millipore, Cat. No. GF156) to suppress the cellular interferon response, and then transfected with the VEE-OKS-iG RNA replicon expressing the reprogramming factors Oct4, Klf4, Sox2 and Glis1. To support iPSC induction, the TeSR™-E7™ reprogramming medium (STEMCELL Technologies, Cat No. 05914) was used until first iPSC colonies became visible; TeSR™-E7™ was then replaced by Essential 8 (E8) medium (Thermo Fisher Scientific). For the generation of Miro1 p.R450C iPSCs, episomal vectors expressing Yamanaka reprogramming factors, namely pCXLE-hUL (Addgene #27080), pCXLE-hSK (Addgene #27078) and pCXLE-hOct3/4 (Addgene #27076), were introduced into patient fibroblasts by electroporation, using the Amaxa Nucleofector II system (Lonza Bioscience) program B16. Transfected cells were plated on Matrigel-coated wells and fed every day with E8 medium. Undifferentiated iPSC colonies were identified by morphology, isolated and expanded; passages were performed every 3–4 days with 0.5 mM EDTA in PBS. Bright field images taken after expansion confirmed the typical iPSC colony morphology for all lines (Fig. 1A).

4.2. Reprogramming vector analysis

Loss of reprogramming vectors was confirmed by PCR using primers specific to the OriP region (Table 2, Supplementary Fig. 1), which is present in all plasmids encoding Yamanaka factors.

4.3. Gene editing

Gene-corrected iPSC lines were generated by Axol Bioscience using the CRISPR/Cas9 technology (Supplementary Fig. 2 and 3). Briefly, iPSCs were co-transfected with the SpCas9 plasmid, the specific gRNA and a single-stranded oligodeoxynucleotide (ssODN) repair template incorporating the corrected allele and also containing synonymous base changes that facilitate PCR screening and prevent Cas9-mediated re-cutting (Table 2, Supplementary Fig. 2 and 3). Cells were then plated on Matrigel-coated wells and fed with mTESR™1 (STEMCELL Technologies).

4.4. PCR and Sanger sequencing

Gene-edited iPSC clones were screened by PCR using the indicated primers (Table 2, Supplementary Fig. 4). PCR amplicons were then sequenced to confirm the successful gene editing and the absence of indel mutations (Table 2, Fig. 1B). Positive clones (clone 18 for Miro1 p.R272Q_GC, clones 6 and 10 for Miro1 p.R450C_GC) were finally expanded and gene correction further confirmed by PCR and sequencing. Location of the corrected alleles and silent mutations introduced are indicated by the hashtags highlighted in red (Fig. 1B).

4.5. Pluripotency assay

Expression of stemness markers was evaluated by both immunocytochemistry (ICC) and RT-qPCR analysis. For the ICC, iPSCs were plated on Matrigel-coated coverslips and fixed in PBS + 4% PFA for 15 min. Cells were then permeabilized and blocked for 1 h in PBS supplemented with 10% goat serum, 2% BSA and 0.4% Triton-X 100, followed by overnight incubation at 4 °C with Nanog and Oct3/4 primary antibodies (Table 2), diluted in 1% goat serum, 0.2% BSA and 0.1% Triton-X 100. The following day, cells were washed in PBS and incubated with the corresponding secondary antibodies (Table 2). Finally, nuclei were stained with Hoechst and images acquired using a Zeiss AxioObserverZ1 microscope (Carl Zeiss Microimaging GmbH). Scale bar = 50 μm (Fig. 1C).

For the RT-qPCR analysis, total RNA was extracted using the RNeasy Mini Kit (QIAGEN) and retrotranscribed using the Transcriptor High Fidelity cDNA Synthesis Kit (Roche). The resulting cDNAs were subjected to multiplex qPCR using the LightCycler® 480 Probes Master Kit (Roche) and the hydrolysis probes NANOG-FAM, OCT3/4-FAM and ACTB-VIC (Table 2). Relative RNA levels were expressed as fold change compared to a wild-type (wt) iPSC line that was used as positive control. cDNA obtained from primary skin fibroblasts was used as negative control (Fig. 1D).

4.6. Three germ layer differentiation

iPSCs were plated on Matrigel-coated coverslips two days before the *in vitro* differentiation procedure started. The Human Pluripotent Stem Cell Functional Identification Kit (R&D Systems, Cat No. SC027B) was used to verify iPSCs capacity to differentiate into the three germ layers. ICC of the ectodermal marker OTX2, the mesodermal marker Brachyury and the endodermal marker SOX17 was performed. Nuclei were stained with Hoechst and images were acquired using a Zeiss AxioObserverZ1 microscope. Scale bar = 50 μm (Fig. 1E).

4.7. Karyotyping and genetic identity

Genomic DNA was isolated from iPSCs and karyotype analysis was performed to exclude the presence of chromosomal aberrations. Karyotype of patient-derived iPSCs (Miro1 p.R272Q and p.R450C mutant lines) was assessed at Life&Brain Genomics (Bonn, Germany) using an Illumina iScan S/N: N234 array (Supplementary Fig. 5, upper panels). Karyotyping of gene-edited lines was performed by Life Technologies (Thermo Fisher Scientific, Madison, WI, USA) using a CytoScan HT-CMA 96F array for Karyostat + analysis (Supplementary Fig. 5, lower panels). Genetic identity between gene-edited and parental lines (both fibroblasts and mutant iPSCs) was confirmed by STR analysis (Cell Line Service, GmbH, Germany, Supplementary Fig. 6).

4.8. Human pathogens analysis

iPSCs were subjected to PCR analysis to exclude the presence of contamination by human pathogens, including Mycoplasma, Hepatitis, HIV and HTLV. All clones resulted negative (Supplementary Fig. 7).

Declaration of Competing Interest

The authors declare that they have no known competing financial interests or personal relationships that could have appeared to influence the work reported in this paper.

Acknowledgements

AC is supported by the Luxembourg Fonds National de Recherche (FNR) within the framework of the PARK-QC DTU (PRIDE17/12244779/PARK-QC). Work of GA is supported by the FNR, grant

number C21/BM/15850547/PINK1-DiaPDs. Work of AG was supported by the FNR within the ATTRACT program (Model-IPD, FNR9631103). RK obtained funding from the FNR PEARL Excellence Programme [FNR/P13/6682797], the Michael J. Fox Foundation, and the European Union's Horizon2020 research and innovation program (WIDESPREAD; CENTRE-PD; grant agreement no. 692320). In addition, RK, AG and GA were supported by the FNR CORE grant MiRisk-PD (C17/BM/11676395).

Appendix A. Supplementary data

Supplementary data to this article can be found online at <https://doi.org/10.1016/j.scr.2023.103145>.

References

- Berenguer-Escuder, C., Grossmann, D., Massart, F., Antony, P., Burbulla, L.F., Glaab, E., Imhoff, S., Trinh, J., Seibler, P., Grünewald, A., Krüger, R., 2019. Variants in Miro1 cause alterations of ER-mitochondria contact sites in fibroblasts from Parkinson's disease patients. *J. Clin. Med.* 8 (12), 2226.
- Berenguer-Escuder, C., Grossmann, D., Antony, P., Arena, G., Wasner, K., Massart, F., et al., 2020. Impaired mitochondrial-endoplasmic reticulum interaction and mitophagy in Miro1-mutant neurons in Parkinson's disease. *Hum. Mol. Genet.* 29, 1353–1364. <https://doi.org/10.1093/hmg/ddaa066>.
- Grossmann, D., Berenguer-Escuder, C., Bellet, M.E., Scheibner, D., Bohler, J., Massart, F., Rapaport, D., Skupin, A., Fouquier d'Hérouël, A., Sharma, M., Ghelfi, J., Raković, A., Lichtner, P., Antony, P., Glaab, E., May, P., Dimmer, K.S., Fitzgerald, J.C., Grünewald, A., Krüger, R., 2019. Mutations in RHOT1 disrupt endoplasmic reticulum-mitochondria contact sites interfering with calcium homeostasis and mitochondrial dynamics in Parkinson's disease. *Antioxid. Redox Signal.* 31 (16), 1213–1234.
- Grossmann, D., Berenguer-Escuder, C., Chemla, A., Arena, G., Krüger, R., 2020. The emerging role of RHOT1/Miro1 in the pathogenesis of Parkinson's disease. *Front. Neurol.* 11, 587. <https://doi.org/10.3389/fneur.2020.00587>.